

# Post-common envelope binaries from SDSS - XVI. Long orbital period systems and the energy budget of CE evolution

A. Rebassa-Mansergas<sup>1</sup>, M. Zorotovic<sup>1</sup>, M.R. Schreiber<sup>1</sup>, B.T. Gänsicke<sup>2</sup>,  
 J. Southworth<sup>3</sup>, A. Nebot Gómez-Morán<sup>4</sup>, C. Tappert<sup>1</sup>, D. Koester<sup>5</sup>, S. Pyrzas<sup>2</sup>,  
 C. Papadaki<sup>6</sup>, L. Schmidtobreick<sup>7</sup>, A. Schwöpe<sup>8</sup>, O. Toloza<sup>1</sup>

<sup>1</sup> *Departamento de Física y Astronomía, Universidad de Valparaíso, Avenida Gran Bretaña 1111, Valparaíso, Chile*

<sup>2</sup> *Department of Physics, University of Warwick, Coventry CV4 7AL, UK*

<sup>3</sup> *Astrophysics Group, Keele University, Staffordshire, ST5 5BG, UK*

<sup>4</sup> *CNRS, Observatoire Astronomique, 11 rue de l'Université, F-67000 Strasbourg, France*

<sup>5</sup> *Institut für Theoretische Physik und Astrophysik, University of Kiel, 24098 Kiel, Germany*

<sup>6</sup> *Institute of Astronomy & Astrophysics, National Observatory of Athens, 15236 Athens, Greece*

<sup>7</sup> *European Southern Observatory, Alonso de Cordova 3107, Santiago, Chile*

<sup>8</sup> *Astrophysikalisches Institut Potsdam, An der Sternwarte 16, D-14482 Potsdam, Germany*

Accepted 2011. Received 2011; in original form 2011

## ABSTRACT

Virtually all close compact binary stars are formed through common-envelope (CE) evolution. It is generally accepted that during this crucial evolutionary phase a fraction of the orbital energy is used to expel the envelope. However, it is unclear whether additional sources of energy, such as the recombination energy of the envelope, play an important role. Here we report the discovery of the second and third longest orbital period post-common envelope binaries (PCEBs) containing white dwarf (WD) primaries, i.e. SDSSJ 121130.94-024954.4 ( $P_{\text{orb}} = 7.818 \pm 0.002$  days) and SDSSJ 222108.45+002927.7 ( $P_{\text{orb}} = 9.588 \pm 0.002$  days), reconstruct their evolutionary history, and discuss the implications for the energy budget of CE evolution. We find that, despite their long orbital periods, the evolution of both systems can still be understood without incorporating recombination energy, although at least small contributions of this additional energy seem to be likely. If recombination energy significantly contributes to the ejection of the envelope, more PCEBs with relatively long orbital periods ( $P_{\text{orb}} \gtrsim 1\text{--}3$  d) harboring massive WDs ( $M_{\text{wd}} \gtrsim 0.8 M_{\odot}$ ) should exist.

**Key words:** Binaries: spectroscopic – stars:low-mass – stars: white dwarfs – binaries: close – stars: post-AGB – stars: evolution variables

## 1 INTRODUCTION

Some of the most interesting objects in our Galaxy are close compact binary stars, such as cataclysmic variables (CVs), low mass X-ray binaries, or double degenerate white dwarf (WD) binaries. The vast majority of close compact binaries form through common envelope (CE) evolution occurring when the more massive star of the initial main sequence binary fills its Roche-lobe on the first giant branch (FGB) or on the asymptotic giant branch (AGB). This may trigger dynamically unstable mass transfer causing the giant's envelope to engulf its core (the future compact object) and the main-sequence companion. Drag forces transfer orbital energy and angular momentum from the binary orbit to the envelope, reducing the binary separation, until eventually

the envelope is expelled and a short orbital period post-common envelope binary (PCEB) consisting of a compact object and a main-sequence companion is exposed.

A commonly used method to predict the outcome of binary star evolution and to theoretically investigate close compact binary star populations are Binary Population Synthesis (BPS) studies which have been performed e.g. for Supernova Type Ia progenitors (Han 2004), short gamma ray bursts (Belczynski et al. 2006), or Galactic WD plus main sequence (WDMS) binaries (Willems & Kolb 2004; Davis et al. 2010). However, in current BPS models CE evolution is commonly approximated by a parametrized energy equation, i.e. a fraction of the available orbital energy, known as the CE efficiency ( $\alpha_{\text{CE}}$ ), is equated to the binding energy of the envelope (Paczynski 1976; Webbink 1984;

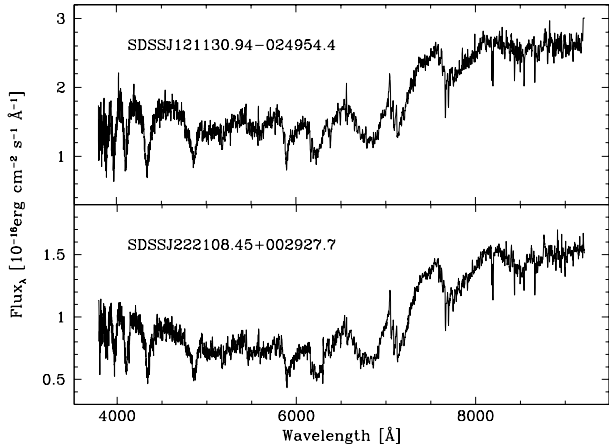


**Figure 1.** SDSS spectra of SDSSJ 1211-0249 and SDSSJ 2221+0029.

Iben & Tutukov 1986; Iben & Livio 1993). While recent observational as well as theoretical results indicate rather small efficiencies for the use of orbital energy, i.e.  $\alpha_{CE} \sim 0.25$  (Zorotovic et al. 2010; Ricker & Taam 2012), it remains unclear if, and to what extent, additional energy sources play an important role in unbinding the envelope.

On the one hand, the long orbital period PCEB IK Peg (Landsman et al. 1993; Vennes et al. 1998) and perhaps also the two symbiotic systems T CrB (Webbink 1976) and RS Oph (Livio et al. 1986) have been claimed to provide direct evidence for additional energy contributions (Davis et al. 2010; Zorotovic et al. 2010) and atomic recombination is often considered to be the most promising candidate (e.g. Webbink 2008). On the other hand, Soker & Harpaz (2003) argue that recombination energy cannot significantly contribute to the ejection process as, according to them, the opacity in the envelope is too small and the energy provided by recombination should be radiated away rather than accelerating the gas.

During the last few years we have successfully identified a large number of PCEBs among WDMS binaries discovered by the Sloan Digital Sky Survey (SDSS, Adelman-McCarthy et al. 2008; Abazajian et al. 2009), and measured the orbital periods of 58 systems (Schreiber et al. 2010; Rebassa-Mansergas et al. 2011; Nebot Gómez-Morán et al. 2011). So far we have found not a single system providing additional direct evidence for recombination energy to be important. As a continuation of this large scale project, we here present orbital period measurements of the PCEBs SDSSJ 121130.94-024954.4 and SDSSJ 222108.45+002927.7 (hereafter SDSSJ 1211-0249 and SDSSJ 2221+0029, see their SDSS spectra in Figure 1) and find these two systems to be the longest orbital period PCEBs in our sample, and currently the second and third longest WDMS PCEBs known after IK Peg. We discuss the implications of these findings for theories of CE evolution with particular emphasis on the possible contributions of recombination energy to the energy budget of CE evolution.

**Table 1.** Log of the observations. Provided are the telescopes and instruments used, and the observing dates (observing periods are provided for the GS and VLT telescopes). The corresponding NTT ESO program ID is 082.D-507(B).

Object SDSSJ	Telescope	Instr.	Date or Obs. Period
1211-0249	GS	GMOS	2008 A and B
	NTT	EFOSC	Mar. 17-25 2009
	M.Baade	IMACS	May 14-16 2009
	M.Baade	IMACS	Dec. 26-29 2009
	VLT	FORS2	085.D-0974(A) (2010)
	VLT	FORS2	087.D-0721(A) (2011)
2221+0029	VLT	FORS2	080.D-0407(A) (2007)
	WHT	ISIS	5-10 Jul. 2008
	CA3.5	TWIN	25-28 Jul. 2008
	CA3.5	TWIN	24-25 Sep. 2009
	VLT	FORS2	085.D-0974(A) (2010)
	VLT	FORS2	087.D-0721(A) (2011)

## 2 OBSERVATIONS

We start with a brief summary of the performed spectroscopic follow-up observations of SDSSJ 1211-0249 and SDSSJ 2221+0029. Instrumentation, data reduction and calibration procedures are identical to those described in Nebot Gómez-Morán et al. (2011). A log of the observations is provided in Table 1.

### 2.1 SDSSJ 1211-0249

SDSSJ 1211-0249 was identified as a PCEB by Nebot Gómez-Morán et al. (2011) based on three  $\text{Na I } \lambda\lambda 8183.27, 8194.81$  absorption doublet radial velocities measurements from GMOS spectra taken at Gemini South (GS) during the semesters 2008 A and B. Additional follow-up spectroscopy aiming to determine the orbital period of SDSSJ 1211-0249 was performed at the New Technology Telescope (NTT) equipped with EFOSC during eight consecutive nights. We took a total of 18 spectra providing radial velocities with rather large uncertainties ( $\sim 20 - 30 \text{ km s}^{-1}$ ) due to relatively poor weather conditions. This first data-set revealed long-term radial velocity variations for SDSSJ 1211-0249. Additional follow-up spectroscopy was performed at Magellan/Baade armed with IMACS during two runs of three and four nights respectively, resulting in five additional radial velocities revealing a promising orbital period estimate of about seven days. However several aliases resulting from integer multiples of a day did not allow a definite determination of the orbital period. Finally, service mode observations at the Very Large Telescope (VLT) UT1 equipped with FORS2 in periods 85 and 87 provided 14 additional radial velocities spanning the entire semesters which broke the alias degeneracy and allowed to accurately measure the orbital period.

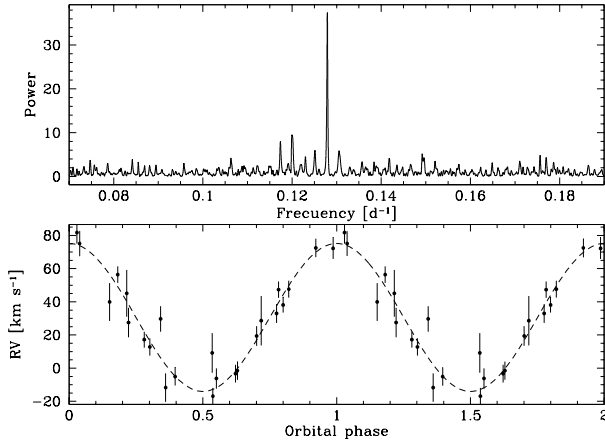


**Figure 2.** Top panel: ORT/TSA periodogram obtained from the radial velocity data of SDSSJ 1211-0249 in Table 2. A clear peak at  $0.128 \text{ d}^{-1}$  can be seen. Bottom panel: the radial velocity curve folded over the period provided by the periodogram in the top panel.

## 2.2 SDSSJ 2221+0029

Based on two spectra obtained with VLT/FORS2 during period 80 we discovered the close binary nature of SDSSJ 2221+0029 (Nebot Gómez-Morán et al. 2011). A first attempt to measure the orbital period was performed with ISIS mounted at the William Herschel Telescope (WHT), where we obtained six spectra. Given the long term trend revealed by the radial velocities derived from these WHT spectra, we obtained seven additional spectra during two observing runs at the 3.5 m telescope at Calar Alto (CA 3.5) equipped with TWIN. However, as in the case of SDSSJ 1211-0249, the short time span of our visitor mode observations provided multiple choices for the orbital period of SDSSJ 2221+0029. We hence obtained service mode observations (20 spectra) at the VLT/FORS2 during periods 85 and 87 that finally allowed to unambiguously determine the orbital period of SDSSJ 2221+0029.

## 3 ORBITAL PERIODS

The data described in Section 2 allow us to accurately determine the orbital periods of SDSSJ 1211-0249 and SDSSJ 2221+0029. Radial velocities were measured in all cases from the Na I  $\lambda\lambda 8183.27, 8194.81$  absorption doublet, in the same fashion as described in Rebassa-Mansergas et al. (2008) and Schreiber et al. (2008). The measured radial velocities are given in Table 2.

A Scargle (1982) periodogram calculated from the radial velocities of SDSSJ 1211-0249 to investigate the periodic nature of the velocity variations contained a number of aliases due to the sampling pattern of the visitor mode observations. Using the ORT/TSA command in MIDAS, which folds and phase-bins the data using a grid of trial periods and fits a series of Fourier terms to the folded radial velocity curve (Schwarzenberg-Czerny 1996), we produced the periodogram shown in the top panel of Figure 2 which reveals a clear peak at  $0.128 \text{ d}^{-1}$ . The same method applied to the

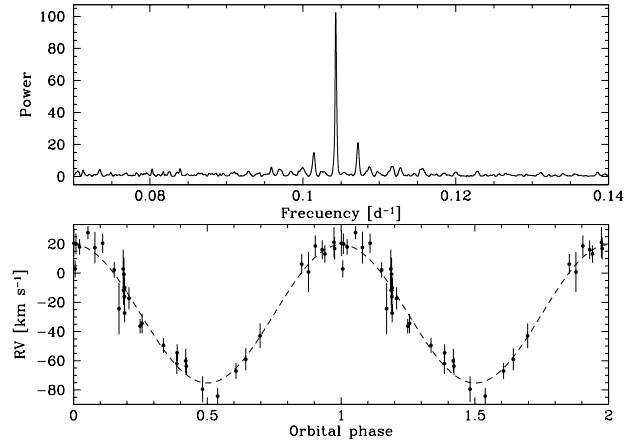


**Figure 3.** Top panel: ORT/TSA periodogram obtained from the radial velocity data of SDSSJ 2221+0029 in Table 2. A clear peak at  $0.104 \text{ d}^{-1}$  can be seen. Bottom panel: the radial velocity curve folded over the period provided by the periodogram in the top panel.

radial velocities of SDSSJ 2221+0029 yields a periodogram with a clear peak at  $0.104 \text{ d}^{-1}$  (top panel of Figure 3).

To obtain a definite value for the orbital periods we finally carried out sine-fits of the form

$$V_r = K_{\text{sec}} \sin \left[ \frac{2\pi(t - T_0)}{P_{\text{orb}}} \right] + \gamma \quad (1)$$

to the radial velocity data sets, where  $\gamma$  is the systemic velocity,  $K_{\text{sec}}$  is the radial velocity semi-amplitude of the companion star,  $T_0$  is the time of inferior conjunction of the secondary star, and  $P_{\text{orb}}$  is the orbital period. We adopted the frequency corresponding to the strongest peaks in the periodograms as the initial orbital period. The parameters resulting from these fits are reported in Table 3 with the orbital periods of SDSSJ 1211-0249 and SDSSJ 2221+0029 being  $7.818 \pm 0.002$  and  $9.588 \pm 0.002$  days respectively. These are the longest orbital periods measured so far in our survey.

## 4 BINARY PARAMETERS

We provide in this Section the binary (orbital and stellar) parameters of the two PCEBs studied in this work. The WD effective temperatures ( $T_{\text{eff(WD)}}$ ), surface gravities ( $\log g_{\text{(WD)}}$ ) and masses ( $M_{\text{wd}}$ ), as well as the secondary star spectral types ( $\text{Sp}_{\text{sec}}$ ), masses and radii ( $M_{\text{sec}}, R_{\text{sec}}$ ) are obtained following the decomposition/fitting technique described in Rebassa-Mansergas et al. (2007). In brief this routine follows a two-step procedure. First, the SDSS spectrum is fitted with a two-component model, and the spectral type of the secondary star is determined (Figure 4). Second, the best-fit M-dwarf is subtracted and the residual WD spectrum is fitted with a model grid of DA WDs (Koester 2010) to determine the WD effective temperature and surface gravity (Figure 5). From an empirical spectral type-radius-mass relation for M-dwarfs (Rebassa-Mansergas et al. 2007) and a mass-radius relation for WDs (Bergeron et al. 1995; Fontaine et al. 2001) we then calculate the mass and radius of the secondary star and the WD respectively.

**Table 2.** Na I radial velocities (RV) and their errors (Rve) measured for SDSSJ 1211-0249 and SDSSJ 2221+0029. Heliocentric Julian dates (HJD) are also provided. The radial velocities are given in  $\text{km s}^{-1}$ .

HJD	RV	Rve	HJD	RV	Rve	HJD	RV	Rve	HJD	RV	Rve	HJD	RV	Rve
SDSSJ1211-0229														
2454510.792206	72.5	5.6	2454642.555408	33.0	5.7	2454644.539962	81.7	6.6	2454911.808350	45.1	14.1	2454915.737374	28.6	14.9
2454966.586407	27.5	8.9	2454967.523802	29.7	7.7	2454967.671370	-11.7	8.6	2455192.758500	39.9	11.4	2455195.755007	9.2	11.9
2455287.587077	17.2	4.8	2455289.592162	-16.9	5.0	2455291.642618	38.1	4.6	2455293.515465	75.1	7.5	2455295.568011	12.8	5.2
2455297.512659	-6.2	6.1	2455299.628209	47.6	5.1	2455306.504832	19.4	5.9	2455660.552464	89.4	11.5	2455665.519683	-3.7	6.8
2455671.572157	-5.5	5.9	2455674.596450	49.1	5.1	2455677.712572	57.5	5.2	2455704.665357	3.7	12.6			
SDSSJ2221+0029														
2454386.661042	27.8	4.5	2454387.598545	2.2	5.3	2454653.712600	8.7	7.2	2454654.647388	0.5	8.7	2454654.719920	0.1	7.1
2454655.676768	0.5	6.6	2454656.622337	-7.2	7.6	2454658.677219	-3.7	5.9	2455329.885273	-0.1	8.3	2455334.874227	3.2	6.0
2455344.812435	6.9	7.6	2455346.823441	2.9	13.2	2455346.834686	-1.7	10.0	2455346.851469	0.7	11.3	2455346.862695	-6.1	11.3
2455354.846936	8.0	5.3	2455357.851973	-9.5	5.0	2455359.794378	-4.3	5.5	2455360.805659	-9.0	7.6	2455382.720068	6.1	6.4
2455385.783274	-6.3	5.0	2455399.671028	-2.9	8.5	2455699.895126	0.4	6.1	2455711.878306	-5.4	9.2	2455720.842993	-5.4	9.0
2455724.834694	-8.9	5.8	2455736.779456	4.4	6.5	2455741.903011	-7.9	5.9	2454672.643400	0.8	13.7	2454673.556708	1.2	10.4
2454674.577014	7.5	10.7	2454675.442195	-4.3	17.5	2454675.641213	-7.4	6.3	2455099.432743	-2.0	7.1	2455100.353820	-9.5	8.8

For the majority of SDSS PCEBs the spectroscopic decomposition results in an uncertainty of the spectral type of  $\pm 0.5$  spectral classes (Rebassa-Mansergas et al. 2010, 2012), and this applies as well to SDSS J2221+0029. However, the SDSS spectrum of SDSS J1211-0249 suffers from low-frequency structure (there is substantial structure left in the residual WD spectrum after the decomposition) that results in a substantially larger uncertainty in the determination of the spectral type of the companion, and correspondingly larger uncertainties in the white dwarf parameters (see left panels of Figure 5 and Table 3). For SDSS J2221+0029,  $M_{\text{wd}}$ ,  $T_{\text{eff(WD)}}$ ,  $\log g_{\text{(WD)}}$ ,  $M_{\text{sec}}$  and  $\text{Sp}_{\text{sec}}$  are obtained by averaging the fit results of two independent SDSS spectra, and the uncertainties are the corresponding standard deviations. For SDSS J1211-0249, we average the parameters over two possible solutions for the spectral decomposition using either an M2 or M3 template, and determine the uncertainties again from the corresponding standard deviations.

To calculate the binary inclinations we use Kepler's third law,

$$\frac{(M_{\text{wd}} \sin i)^3}{(M_{\text{wd}} + M_{\text{sec}})^2} = \frac{P_{\text{orb}} K_{\text{sec}}^3}{2\pi G} \quad (2)$$

rewritten as

$$\sin i = \frac{K_{\text{sec}}}{M_{\text{wd}}} \left( \frac{P_{\text{orb}}}{2\pi G} \right)^{1/3} (M_{\text{wd}} + M_{\text{sec}})^{2/3}, \quad (3)$$

with the orbital periods and semi-amplitude velocities of the companions  $K_{\text{sec}}$  as determined in Section 3, and the stellar masses as obtained from the analysis of the SDSS spectra outlined above. The well known relation  $M_{\text{sec}}/M_{\text{wd}} = K_{\text{wd}}/K_{\text{sec}} = q$  provides an estimate of the expected semi-amplitude velocity of the WD  $K_{\text{wd}}$ . Finally, estimates of the orbital separations and Roche lobe radii of the secondary stars  $R_{\text{Lsec}}$  are obtained from Kepler's third law and Eggleton's (1983) expression

$$R_{\text{Lsec}} = \frac{a 0.49 q^{2/3}}{0.6 q^{2/3} + \ln(1 + q^{1/3})} \quad (4)$$

respectively. The complete sets of binary parameters for

**Table 3.** Binary parameters obtained for SDSSJ 1211-0249 and SDSSJ 2221+0029.  $M_{\text{wd}}$ ,  $M_{\text{sec}}$ ,  $R_{\text{sec}}$ , spectral type of the companion  $\text{Sp}_{\text{sec}}$ ,  $T_{\text{eff(WD)}}$  and  $\log g$  are obtained following the decomposition/fitting routine described in Rebassa-Mansergas et al. (2007). The orbital period  $P_{\text{orb}}$ , the secondary star semi-amplitude  $K_{\text{sec}}$ , and the systemic velocity  $\gamma_{\text{sec}}$  are measured in Section 3. Estimates of the orbital separation  $a$ , mass ratio  $q$ , white dwarf semi-amplitude velocity  $K_{\text{wd}}$ , secondary Roche lobe radius  $R_{\text{Lsec}}$ , and inclination are obtained from the equations given in Section 4.

	SDSS J1211-0229		SDSS J2221+0029	
$M_{\text{wd}} [M_{\odot}]$	0.52	$\pm$ 0.07	0.54	$\pm$ 0.03
$M_{\text{sec}} [M_{\odot}]$	0.41	$\pm$ 0.05	0.38	$\pm$ 0.07
$q$	0.79	$\pm$ 0.15	0.70	$\pm$ 0.15
$a [R_{\odot}]$	16.2	$\pm$ 0.5	18.5	$\pm$ 0.5
$P_{\text{orb}} [\text{d}]$	7.818	$\pm$ 0.002	9.588	$\pm$ 0.002
$\gamma_{\text{sec}} [\text{km s}^{-1}]$	30	$\pm$ 2	-29	$\pm$ 2
$K_{\text{sec}} [\text{km s}^{-1}]$	44	$\pm$ 3	49	$\pm$ 2
$K_{\text{wd}} [\text{km s}^{-1}]$	35	$\pm$ 7	34	$\pm$ 7
$\text{Sp}_{\text{sec}}$	M2.5	$\pm$ 1	M3	$\pm$ 0.5
$R_{\text{sec}} [R_{\odot}]$	0.42	$\pm$ 0.05	0.39	$\pm$ 0.08
$R_{\text{sec}}/R_{\text{Lsec}}$	0.07	$\pm$ 0.01	0.06	$\pm$ 0.01
$i [^{\circ}]$	49	$\pm$ 7	58	$\pm$ 7
$T_{\text{eff(WD)}} [\text{K}]$	13130	$\pm$ 860	18440	$\pm$ 150
$\log g_{\text{(WD)}}$	7.84	$\pm$ 0.13	7.85	$\pm$ 0.06

SDSSJ 1211-0249 and SDSSJ 2221+0029 are given in Table 3.

## 5 DISCUSSION

We have presented in the previous Sections the discovery of the second and third longest orbital period (detached) PCEBs containing a WD primary. In what follows we reconstruct the evolutionary history of both systems and discuss implications for our understanding of CE evolution.

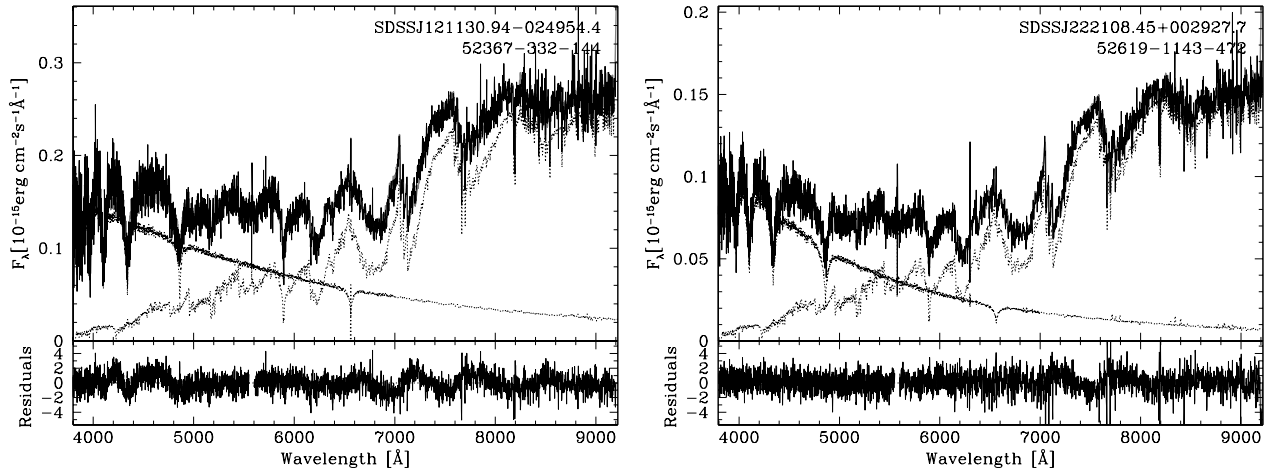


**Figure 4.** Two-component fit to the spectra of SDSSJ 1211+0249 (left) and SDSSJ 2221+0029 (right). The top panels show the spectra of the objects as a solid black lines and the two templates, white dwarf and M-dwarf, as dotted lines. The bottom panel shows the residuals from the fit. SDSS MJD, PLT and FIB identifiers are also indicated.

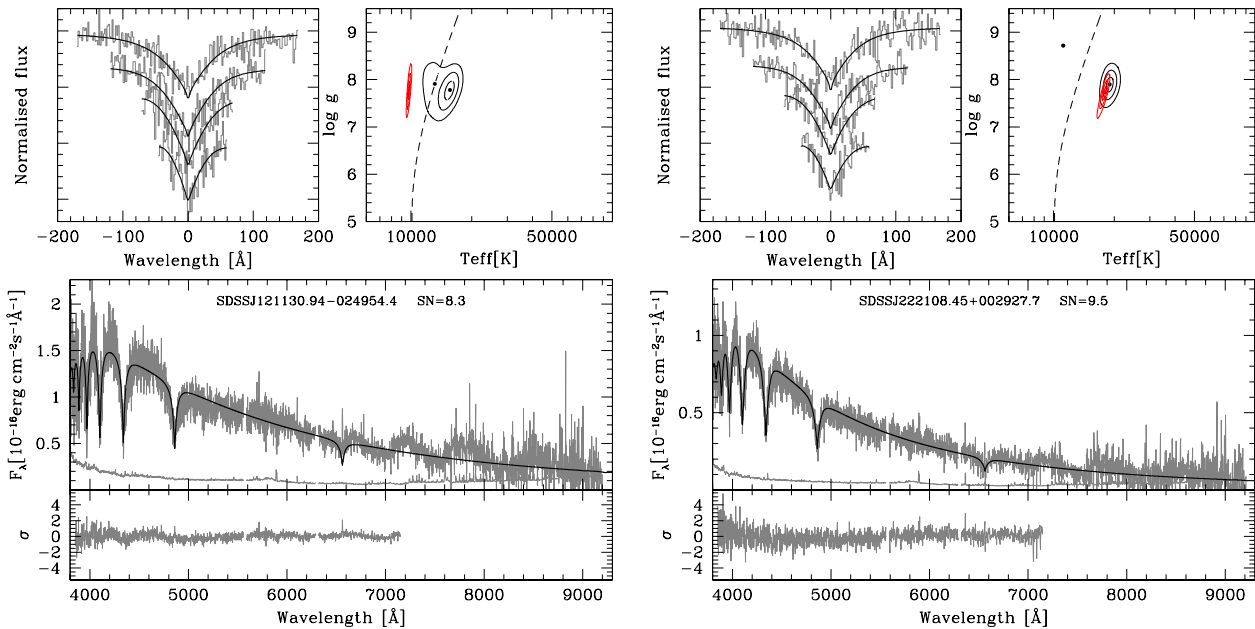


**Figure 5.** Spectral model fit to the white dwarf in SDSSJ 1211+0249 and SDSSJ 2221+0029, obtained after subtracting the best-fit M-dwarf templates (see Figure 4). Top left panels: best-fit (black lines) to the observed H $\beta$  to He (gray lines, top to bottom) line profiles. The model spectra and observations have been normalised in the same way. Top right panels: 1, 2 and 3  $\sigma$  contour plots in the  $T_{\text{eff}}-\log g$  plane. The black contours refer to the best line profile fit, the red ones (which collapse into a dot on the scale of the plot) to the fit of the spectral range 3850–7150  $\text{\AA}$ . The dashed line indicates the occurrence of maximum H $\beta$  equivalent width. The best “hot” and “cold” line profile solutions are indicated by black dots, while the best fit to the whole spectrum by a red one. Bottom panels: the residual white dwarf spectra resulting from the spectral decomposition and their flux errors (gray lines) along with the best-fit white dwarf model (black lines) in the 3850–7150  $\text{\AA}$  wavelength range (top) and the residuals of the fit (gray line, bottom).

### 5.1 The evolution of SDSSJ 1211-0249 and SDSSJ 2221+0029

Having at hand the orbital periods, the stellar mass estimates of both components and the WD effective temperatures allows us to reconstruct the evolutionary history of SDSSJ 1211-0249 and SDSSJ 2221+0029 and predict their future following Zorotovic et al. (2011) and Schreiber & Gänsicke (2003) respectively. First, we

interpolate the cooling tracks of Wood (1995) and Althaus & Benvenuto (1997) to determine the cooling age of both systems. Second, we derive the orbital period at the end of the CE phase using the the most up-to-date version of disrupted magnetic braking (Hurley et al. 2002, including the normalization provided by Davis et al. 2008). Third, we use the single-star evolution (SSE) code of Hurley et al. (2000) to reconstruct the CE phase for a given value of the

**Table 4.** Applying the reconstruction algorithm described in Zorotovic et al. (2011) we determine the orbital periods at the end of CE evolution  $P_{\text{CE}}$ , the initial mass of the primary  $M_{1,\text{o}}$ , the mass of the primary at the onset of CE evolution  $M_{1,\text{CE}}$ , the corresponding orbital separation  $a_i$ , the main sequence lifetime of the primary  $t_{\text{evolV}}$ , the cooling age of the WD  $t_{\text{cool}}$ , and the time until the second phase of mass transfer will occur from now on  $t_{\text{sd}}$  and since the progenitor main sequence binary has formed  $t_{\text{tot}}$ . Columns two and four correspond to a fixed value of  $\alpha_{\text{CE}} = 0.25$ . Columns three and five give the entire range of possible solutions. Note that since disrupted magnetic braking is very inefficient for long orbital period systems,  $P_{\text{CE}}$  is nearly identical to  $P_{\text{orb}}$  in Table 3.

	SDSS J1211-0229		SDSS J2221+0029	
$\alpha_{\text{CE}}$	0.25	0.03-1	0.25	0.06-1
$P_{\text{CE}}$ [d]	7.820	7.819-7.822	9.589	9.588-9.589
$M_{1,\text{o}}$ [ $M_{\odot}$ ]	1.31	0.98-2.35	1.44	1.31-2.35
$M_{1,\text{CE}}$ [ $M_{\odot}$ ]	1.1	0.8-2.3	1.2	1.0-2.3
$a_i$ [ $R_{\odot}$ ]	480.8	246.2-613.9	512.2	295.5-611.3
$P_{\text{sd}}$ [h]	26.0	24.0-28.2	32.0	28.9-36.0
$t_{\text{evolV}}$ [Gyr]	4.82	0.95-13.29	3.53	0.95-4.82
$t_{\text{cool}}$ [Gyr]	0.24	0.24-0.43	0.08	0.07-0.09
$t_{\text{sd}}$ [Gyr]	225.3	140.1-339.7	268.5	150.13-454.36
$t_{\text{tot}}$ [Gyr]	230.4	141.3-353.4	272.1	151.15-459.27

CE efficiency and obtain the orbital and stellar parameters prior to CE evolution.

We here follow Zorotovic et al. (2010) and *assume* that recombination energy contributes to expelling the envelope with the same efficiency as the orbital energy (given by  $\alpha_{\text{CE}}$ ) and take into account the uncertainties in the stellar component masses and WD effective temperatures. We obtain solutions for rather large ranges of the CE efficiency for both systems that are given together with the resulting range of possible parameters and evolutionary time scales of the progenitor system in Table 4. As outlined in the introduction, there seems to be some evidence for a relatively small CE efficiency and we therefore additionally provide the progenitor parameters assuming  $\alpha_{\text{CE}} = 0.25$  in Table 4 (the uncertainties of the stellar masses and WD effective temperature are not considered here). This complements the results presented in Zorotovic et al. 2011 (their Table 3). Given that magnetic braking is not efficient in long orbital period systems, the current orbital periods (Table 3) are nearly identical to those at the end of the CE phase. The masses of the reconstructed progenitors for both objects are similar, which is not surprising since the available estimates of the stellar masses are quite similar too.

Since the current orbital periods of SDSSJ 1211-0249 and SDSSJ 2221+0029 are very long for PCEBs, the stellar components will not be close enough to trigger the second phase of mass transfer before the secondaries in both systems evolve away from the main sequence. Both secondaries will therefore fill their Roche lobes during the FGB transforming SDSSJ 1211-0249 and SDSSJ 2221+0029 into symbiotic systems with stable mass transfer from a red giant to a white dwarf. This is supposed to happen in many Hubble times when the orbital periods have shrunk to  $\sim 1-1.5$  days.

## 5.2 The energy budget of CE evolution

In their review, Iben & Livio (1993) describe several energy sources apart from orbital energy that might contribute to expelling the envelope, ranging from recombination energy to dust driven winds. Since the writing of this review, the energy equation of CE evolution in general, and especially the potential importance of recombination energy, has been a matter of debate (e.g. Dewi & Tauris 2000; Webbink 2008; Xu & Li 2010; Loveridge et al. 2011; Soker & Harpaz 2003; Zorotovic et al. 2010).

In the previous Section we reconstructed the evolution of the long orbital period PCEBs SDSSJ 1211-0249 and SDSSJ 2221+0029 *assuming* that recombination energy contributes to expelling the envelope with the same efficiency as the orbital energy and found large ranges of possible solutions. Here we investigate whether this assumed additional energy is a necessary ingredient to understand the evolutionary history of SDSSJ 1211-0249 and SDSSJ 2221+0029. To that end we now reconstruct the CE phase of both systems without considering recombination energy. Taking into account the uncertainty of the measured stellar parameters, we find possible progenitors for both systems without violating energy conservation, i.e.  $\alpha_{\text{CE}} = 0.21-1$  for SDSSJ 1211-0249 and  $\alpha_{\text{CE}} = 0.42-1$  for SDSSJ 2221+0029. We therefore conclude that the existence of the two systems does not confirm or disprove whether recombination (or any other additional) energy plays an important role during the CE phase. However, the current configuration of SDSSJ 2221+0029 can only be explained if a relatively large fraction of the released orbital energy contributes to envelope ejection, i.e.  $\alpha_{\text{CE}} > 0.42$ . This value exceeds the estimates given in recent studies of CE evolution that seem to converge towards a CE efficiency of  $\alpha_{\text{CE}} \sim 0.25$  (Zorotovic et al. 2010; Ricker & Taam 2012; Passy et al. 2012). If this is generally true, at least a small fraction of recombination energy (or any other form of additional energy) seems to have contributed to the envelope ejection in SDSSJ 2221+0029. Although this interpretation appears tempting, the fact remains that not a single PCEB within the homogeneous SDSS sample (Nebot Gómez-Morán et al. 2011) provides *direct* evidence for additional sources of energy playing a role during CE evolution.

## 5.3 Future perspectives

IK Peg has been highlighted as a key object as it is the longest orbital period system and contains the most massive secondary star among the known PCEBs containing a white dwarf primary. IK Peg requires extra energy that helps to expel the envelope during CE evolution (e.g. Davis et al. 2010). Indeed, IK Peg cannot be reconstructed unless at least a small fraction of recombination energy is taken into account (Zorotovic et al. 2010). In contrast to IK Peg the two PCEBs discussed here, SDSSJ 1211-0249 and SDSSJ 2221+0029, contain relatively low-mass C/O-core WDs (Table 3), therefore their progenitors filled their Roche lobes early on the AGB, i.e. when the envelope was not very extended. Recombination energy, however, is expected to be most important when the WD progenitor radius is large and the envelope is loosely bound (Webbink 2008). The peculiarity of IK Peg is therefore not only its

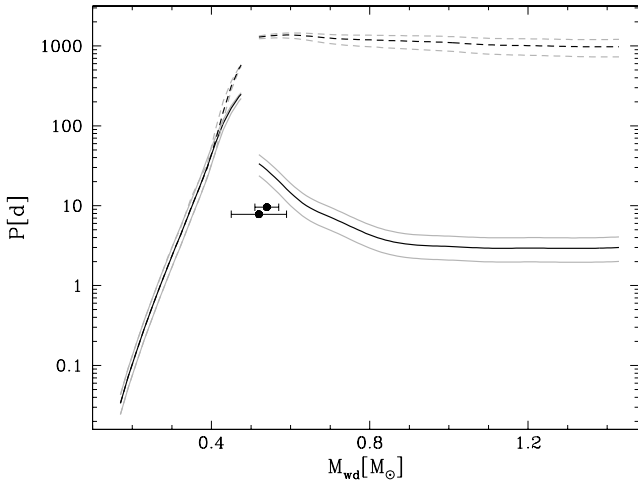


**Figure 6.** Maximum orbital period versus WD mass assuming a secondary star mass of  $M_{\text{sec}} = 0.4 \pm 0.1 M_{\odot}$  (gray lines). The dashed lines correspond to the maximum orbital period if all recombination energy goes into CE ejection, while the solid lines provides the same limit but without taking into account possible contributions from recombination. Any system located between the two lines would provide direct evidence for the contributions of recombination energy. The difference between both lines is largest for high mass WDs as the relative importance of recombination energy increases on the AGB. So far all PCEBs in the homogeneous SDSS sample lie well below the solid lines. Note that the exact location of the two lines depends on the secondary star mass. PCEBs with more massive secondaries have more orbital energy available and the limits are hence slightly shifted towards longer orbital periods.

long orbital period but also the high mass of its WD, which implies that the system entered the CE phase when the radius of the primary was very large on the AGB, a peculiarity our two PCEBs do not share.

To predict which kind of PCEBs would provide the desired direct evidence for contributions of recombination energy we once more use the reconstruction algorithm described in Zorotovic et al. (2011). As usual we assume that the WD mass is equal to the core mass of the giant progenitor at the onset of mass transfer and that the secondary star mass remains constant during CE evolution. For a given core mass we use the SSE code from Hurley et al. (2000) to calculate all possible progenitor masses and their radii. As the radius of the progenitor must have been equal to the Roche radius at the onset of CE evolution we obtain the initial separation for given white dwarf and main sequence companion masses, leaving the final orbital period and the CE efficiency as the remaining free parameters connected via the energy equation. For each progenitor mass the solution with  $\alpha_{\text{CE}} \simeq 1.0$  corresponds to the longest possible final orbital period not violating energy conservation. Among these possible solutions we finally can select the maximum orbital period for a given combination of white dwarf and secondary star masses.

In Figure 6 we show the resulting PCEB maximum orbital period as a function of WD mass assuming a fixed secondary star mass of  $M_{\text{sec}} = 0.4 \pm 0.1 M_{\odot}$ . The positions of SDSSJ 1211-0249 and SDSSJ 2221+0029 are indicated by black solid dots. The dashed lines have been obtained by assuming that all the available recombination energy goes into

envelope ejection while the solid lines represent the maximum orbital period if the envelope is expelled by the use of orbital energy only. The upper and lower (solid and dashed) gray lines correspond to  $M_{\text{sec}} = 0.5 M_{\odot}$  and  $M_{\text{sec}} = 0.3 M_{\odot}$  respectively. The orbital period limits increase with the secondary star mass because PCEBs with more massive secondaries have more orbital energy available.

Any PCEB located above the solid line in Figure 6 (for a given secondary star mass) would provide direct evidence for contributions of additional energy sources. Apparently, recombination energy as the most likely extra-energy can only be important on the tip of the FGB and on the AGB (see dashed lines in Figure 6). For high mass WDs ( $M_{\text{wd}} \gtrsim 0.8 M_{\odot}$ ) the range of orbital periods that would provide evidence for recombination energy is significantly shifted towards shorter (easily measurable) orbital periods of a few days. However, so far not a single known PCEB apart from IK Peg has a relatively long orbital period *and* contains a high-mass WD. The seven SDSS PCEBs with accurately determined orbital periods and stellar parameters containing massive WDs ( $\geq 0.8 M_{\odot}$ ) have orbital periods shorter than one day (see Table 3 in Zorotovic et al. 2011). This might further indicate that the fraction of recombination energy going into envelope ejection is small. However, further observational constraints are required to confirm this supposition. We have therefore just started an observing campaign to measure orbital periods of additional SDSS PCEBs with  $M_{\text{wd}} \gtrsim 0.8 M_{\odot}$  to further constrain the importance of recombination energy during CE evolution. The secondary star masses of the PCEBs in our SDSS follow-up project are mostly in the range of  $M_{\text{sec}} \sim 0.2 - 0.4 M_{\odot}$  which corresponds to orbital period limits given by the full use of orbital energy of  $\sim 1 - 3$  days (see Figure 6). Direct evidence for additional energy, most likely from recombination, would be provided if at least one system will be found to have a period exceeding this limit. If in contrast no such system will be detected, the contribution of recombination energy during CE evolution is likely of minor importance.

## 6 CONCLUSION

We have measured the orbital periods of SDSSJ 1211-0249 and SDSSJ 2221+0029 to be  $7.818 \pm 0.002$  and  $9.588 \pm 0.002$  days respectively. This makes them the longest orbital period PCEBs containing a WD primary and main sequence companion after the well known record holder IK Peg. We reconstructed the CE evolution of both systems taking into account and ignoring additional sources of energy. Although no direct evidence for contributions of recombination energy during CE evolution is provided, it appears plausible that at least a small fraction of this energy helped expelling the envelope. Measuring the orbital periods of more PCEBs containing high-mass ( $M_{\text{wd}} \gtrsim 0.8 M_{\odot}$ ) WDs will provide further constraints on the importance of recombination energy during CE evolution.

## ACKNOWLEDGMENTS

ARM acknowledges financial support from Fondecyt in the form of grant number 3110049. MZ acknowledges sup-

port from Gemini/Conicyt, grant number 32100026. MRS acknowledges support from Milenium Science Initiative, Chilean Ministry of Economy, Nucleus P10-022-F, and Fondecyt (1061199). ANGM acknowledges support by the Centre National d'Etudes Spatial (CNES, ref. 60015). This project was supported in part by the DFHG under contract Schw536/33-1. We also thank the anonymous referee for his/her suggestions that helped improving the quality of the paper.

The presented research is based on observations collected at the following telescopes: the European Organisation for Astronomical Research in the Southern Hemisphere, Chile (080.D-0407(A), 082.D-0507(B)) 085.D-0974(A), 087.D-0721(A)); the Gemini Observatory, which is operated by the Association of Universities for Research in Astronomy, Inc., under a cooperative agreement with the NSF on behalf of the Gemini partnership: the National Science Foundation (United States), the Science and Technology Facilities Council (United Kingdom), the National Research Council (Canada), CONICYT (Chile), the Australian Research Council (Australia), Ministério da Ciência e Tecnologia (Brazil) and Ministerio de Ciencia, Tecnología e Innovación Productiva (Argentina) (GS-2008A-Q-31, GS-2008B-Q-40); the Magellan Baade Telescope located at Las Campanas Observatory, Chile; the William Herschel Telescope, operated on the island of La Palma by the Isaac Newton Group in the Spanish Observatorio del Roque de los Muchachos of the Instituto de Astrofísica de Canarias; and at the Centro Astronómico Hispano Alemán (CAHA) at Calar Alto, operated jointly by the Max-Planck Institut für Astronomie and the Instituto de Astrofísica de Andalucía.

## REFERENCES

- Abazajian, K. N., et al., 2009, *ApJ*, 182, 543  
 Adelman-McCarthy, J. K., et al., 2008, *ApJS*, 175, 297  
 Althaus, L. G., Benvenuto, O. G., 1997, *ApJ*, 477, 313  
 Belczynski, K., Perna, R., Bulik, T., Kalogera, V., Ivanova, N., Lamb, D. Q., 2006, *ApJ*, 648, 1110  
 Bergeron, P., Wesemael, F., Beauchamp, A., 1995, *PASP*, 107, 1047  
 Davis, P. J., Kolb, U., Willems, B., Gänsicke, B. T., 2008, *MNRAS*, 389, 1563  
 Davis, P. J., Kolb, U., Willems, B., 2010, *MNRAS*, 403, 179  
 Dewi, J. D. M., Tauris, T. M., 2000, *A&A*, 360, 1043  
 Eggleton, P. P., 1983, *ApJ*, 268, 368  
 Fontaine, G., Brassard, P., Bergeron, P., 2001, *PASP*, 113, 409  
 Han, Z. and Podsiadlowski, P., 2004, *MNRAS*, 350, 1301  
 Hurley, J. R., Pols, O. R., Tout, C. A., 2000, *MNRAS*, 315, 543  
 Hurley, J. R., Tout, C. A., Pols, O. R., 2002, *MNRAS*, 329, 897  
 Iben, Jr., I., Tutukov, A. V., 1986, *ApJ*, 311, 742  
 Iben, I. J., Livio, M., 1993, *PASP*, 105, 1373  
 Koester, D., 2010, *Memorie della Societa Astronomica Italiana*, 81, 921  
 Landsman, W., Simon, T., Bergeron, P., 1993, *PASP*, 105, 841  
 Livio, M., Truran, J. W., Webbink, R. F., 1986, *ApJ*, 308, 736  
 Loveridge, A. J., van der Sluys, M. V., Kalogera, V., 2011, *ApJ*, 743, 49  
 Nebot Gómez-Morán, A., et al., 2011, *A&A*, 536, A43  
 Paczynski, B., 1976, in P. Eggleton, S. Mitton, & J. Whelan, ed., *Structure and Evolution of Close Binary Systems*, vol. 73 of *IAU Symposium*, p. 75  
 Passy, J.-C., et al., 2012, *ApJ*, 744, 52  
 Rebassa-Mansergas, A., Gänsicke, B. T., Rodríguez-Gil, P., Schreiber, M. R., Koester, D., 2007, *MNRAS*, 382, 1377  
 Rebassa-Mansergas, A., Gänsicke, B. T., Schreiber, M. R., Koester, D., Rodríguez-Gil, P., 2010, *MNRAS*, 402, 620  
 Rebassa-Mansergas, A., Nebot Gómez-Morán, A., Schreiber, M. R., Gänsicke, B. T., Schwöpe, A., Gallardo, J., Koester, D., 2012, *MNRAS*, 419, 806  
 Rebassa-Mansergas, A., Nebot Gómez-Morán, A., Schreiber, M. R., Girven, J., Gänsicke, B. T., 2011, *MNRAS*, 413, 1121  
 Rebassa-Mansergas, A., et al., 2008, *MNRAS*, 390, 1635  
 Ricker, P. M., Taam, R. E., 2012, *ApJ*, 746, 74  
 Scargle, J. D., 1982, *ApJ*, 263, 835  
 Schreiber, M. R., Gänsicke, B. T., 2003, *A&A*, 406, 305  
 Schreiber, M. R., Gänsicke, B. T., Southworth, J., Schwöpe, A. D., Koester, D., 2008, *A&A*, 484, 441  
 Schreiber, M. R., et al., 2010, *A&A*, 513, L7+  
 Schwarzenberg-Czerny, A., 1996, *ApJ Lett.*, 460, L107  
 Soker, N., Harpaz, A., 2003, *MNRAS*, 343, 456  
 Vennes, S., Christian, D. J., Thorstensen, J. R., 1998, *ApJ*, 502, 763  
 Webbink, R. F., 1976, *Nature*, 262, 271  
 Webbink, R. F., 1984, *ApJ*, 277, 355  
 Webbink, R. F., 2008, in E. F. Milone, D. A. Leahy, & D. W. Hobill, ed., *Astrophysics and Space Science Library*, vol. 352 of *Astrophysics and Space Science Library*, p. 233  
 Willems, B., Kolb, U., 2004, *A&A*, 419, 1057  
 Wood, M. A., 1995, in D. Koester & K. Werner, ed., *White Dwarfs*, vol. 443 of *Lecture Notes in Physics*, Berlin Springer Verlag, p. 41  
 Xu, X.-J., Li, X.-D., 2010, *ApJ*, 716, 114  
 Zorotovic, M., Schreiber, M. R., Gänsicke, B. T., Nebot Gómez-Morán, A., 2010, *A&A*, 520, A86  
 Zorotovic, M., Schreiber, M. R., Gänsicke, B. T., 2011, *A&A*, 536, A42